Interactions of 1 um latex microbeads with biofilms
by William Joseph Drury

A thesis submitted in partial fulfillment of the requirements for the degree of Doctor of Philosophy in Civil Engineering
Montana State University

Abstract:
Fluorescently-labelled latex microbeads were used to study the interaction of particles with Pseudomonas aeruginosa biofilms in a continuous flow annular reactor. Microbeads could be readily identified and distinguished from bacteria under the microscope in both plan and cross-section views. Microbeads concentrations were quantifiable. The fraction of beads that attached to biofilm during a 24 h period ranged from 0.001 to 0.01 and was proportional to biofilm cell carbon and standard deviation in biofilm thickness. Microbeads formed aggregates on the biofilm, but not in the associated bulk water. Microbeads added to biofilm of steady state thickness (30 μm) were observed to be located throughout the entire biofilm depth in 24 hours. It was hypothesized that pores in biofilm permitted beads to enter the biofilm interior. Bacterial growth filled in the pores, trapping beads beneath them. Many of the microbeads that attached to biofilm shortly after bacterial inoculation (thickness of 2 μm) remained near the substratum as cells grew past and covered them. Whether added to mature or nascent biofilms, microbeads were observed near the biofilm-substratum interface for up to five days after bead addition. Microbeads were retained by biofilm for longer periods (120 hours) than the average retention experienced by suspended beads in the reactor (0.25 hours), suggesting differences between biofilm and suspended cell ecology. Microbeads located at or near the substratum were released more slowly than were beads nearer to the biofilm-bulk water interface. The bead release rate (0.028 h^-1) was lower than the average cellular growth rate (0.15 h^-1). Model predictions of particle locations and detachment rates by a onedimensional model (BIOSIM) were poor. It was hypothesized that the roughness of the biofilm surface directed particle advection parallel as well as perpendicular to the substratum. This could have been responsible for the inaccuracy of the one-dimensional model. Collectively, these results point to an important role of biofilm roughness in determining particle capture and retention by biofilms.

INTERACTIONS OF 1 μm LATEX MICROBEADS WITH BIOFILMS

by

William Joseph Drury

A thesis submitted in partial fulfillment
of the requirements for the degree

of

Doctor of Philosophy

in

Civil Engineering

MONTANA STATE UNIVERSITY
Bozeman, Montana

August 1992

D378
D8455

APPROVAL

of a thesis submitted by

William Joseph Drury

This thesis has been read by each member of the thesis committee and has been found to be satisfactory regarding content, English usage, format, citations, bibliographic style, and consistency, and is ready for submission to the College of Graduate Studies.

August 11, 1992 — Philip A. Stewart

Date — Chairperson, Graduate Committee

Approved for the Major Department

11 August 1992 — Lewdae E. Long

Date — Head, Major Department

Approved for the College of Graduate Studies

8/28/92 — RL Brown

Date — Graduate Dean

STATEMENT OF PERMISSION TO USE

In presenting this thesis in partial fulfillment of the requirements for a doctoral degree at Montana State University, I agree that the Library shall make it available to borrowers under rules of the Library. I further agree that copying is allowable only for scholarly purposes, consistent with "fair use" as prescribed in the U.S. Copyright Law. Requests for extensive copying or reproduction of this thesis should be referred to University Microfilms International, 300 North Zeeb Road, Ann Arbor, Michigan 48106, to whom I have granted "the exclusive right to reproduce and distribute copies of the dissertation in and from microfilm and the right to reproduce and distribute by abstract in any format."

Signature William J. Drury

Date September 6, 1992

ACKNOWLEDGEMENTS

It would be misleading to present this research as totally the effort of one individual. Therefore, I wish to thank those who participated and helped me complete this goal in my life.

The late Bill Characklis deserves the most thanks for his guidance and patience. I dedicate this thesis to his memory. Phil Stewart is thanked for the advice and ideas given to me. Al Cunningham, Zbigniew Lewandowski, Gordon McFeters, and Ron Larsen are my other committee members who are thanked for their contributions.

I especially thank Paul Stoodley, Anne Camper, Gary Harkin, and Shawn Handran for their assistance. Additional faculty and staff who made contributions are Warren, Gill, Paul, Marty, John, Dave, Bryan, Frank, Whon Chee, Peg, Sandy, Diane, Wendy, Jamie, Cheryl, Susan, Lynda, Cheryl, Nick, Kim, Jordan, Phil, Brian, Jason, Bill, Ralf, and Mary. I also thank Gayle Callis, Gordon Williamson, and Oskar Wanner.

The students who helped me are almost too numerous to mention. I am most thankful to Brent Peyton and Ewout van der Wende. I also thank Satoshi, Robert, Vivek, Gabi, Feisal, Paul, Ross, Thomas, Ernie, Kirk, Leora, Wendy, Sandor, Rick, Barbara, and Rick.

I thank the National Science Foundation for financial support.

TABLE OF CONTENTS

TABLE OF CONTENTS - Continued

LIST OF TABLES

LIST OF TABLES - continued

LIST OF TABLES - continued

LIST OF FIGURES

LIST OF FIGURES - Continued

LIST OF FIGURES - Continued

ABSTRACT

Fluorescently-labelled latex microbeads were used to study the interaction of particles with *Pseudomonas aeruginosa* biofilms in a continuous flow annular reactor. Microbeads could be readily identified and distinguished from bacteria under the microscope in both plan and cross-section views. Microbeads concentrations were quantifiable. The fraction of beads that attached to biofilm during a 24 h period ranged from 0.001 to 0.01 and was proportional to biofilm cell carbon and standard deviation in biofilm thickness. Microbeads formed aggregates on the biofilm, but not in the associated bulk water. Microbeads added to biofilm of steady state thickness (30 μm) were observed to be located throughout the entire biofilm depth in 24 hours. It was hypothesized that pores in biofilm permitted beads to enter the biofilm interior. Bacterial growth filled in the pores, trapping beads beneath them. Many of the microbeads that attached to biofilm shortly after bacterial inoculation (thickness of 2 μm) remained near the substratum as cells grew past and covered them. Whether added to mature or nascent biofilms, microbeads were observed near the biofilm-substratum interface for up to five days after bead addition. Microbeads were retained by biofilm for longer periods (120 hours) than the average retention experienced by suspended beads in the reactor (0.25 hours), suggesting differences between biofilm and suspended cell ecology. Microbeads located at or near the substratum were released more slowly than were beads nearer to the biofilm-bulk water interface. The bead release rate (0.028 h^{-1}) was lower than the average cellular growth rate (0.15 h^{-1}). Model predictions of particle locations and detachment rates by a one-dimensional model (BIOSIM) were poor. It was hypothesized that the roughness of the biofilm surface directed particle advection parallel as well as perpendicular to the substratum. This could have been responsible for the inaccuracy of the one-dimensional model. Collectively, these results point to an important role of biofilm roughness in determining particle capture and retention by biofilms.

INTRODUCTION

A biofilm has been defined as a film consisting of cells immobilized at a substratum and frequently embedded in an extracellular organic polymer (EPS) matrix of microbial origin (Characklis and Marshall, 1990). Biofilms may contain inorganic particles, such as clays, silts, corrosion products, or organic colloids, all of which are retained by the EPS matrix. Microorganisms and EPS may themselves be viewed as particulate constituents of biofilms. Interactions between particles and biofilms represent processes that affect biofilm structure, chemistry, and ecology significantly.

One important particle-biofilm interaction is the capture of particles from the bulk liquid. For example, the filamentous surface of a rotating biological contactor (RBC) biofilm entrapped particles such as organic solids (Alleman *et al.*, 1982). Reactor geometry influences particle capture by biofilms because it affects the surface area available for deposition of solids by gravity or interception of particles in the bulk flow (Bouwer, 1987). Biofilm grown on granular activated carbon (GAC) improved the capture of colloidal particles over clean GAC (Sprouse and Rittman, 1990). Many substrates in natural systems exist as colloidal particles (Levine *et al.*, 1985). Capture of such substrates could increase biofilm growth over that produced by soluble substrates alone. Capture of suspended microorganisms could introduce new species to a biofilm.

Inorganic particles may be captured by or formed in biofilms. Corrosion products are examples of particles produced within a biofilm by microbially influenced corrosion. Inorganic corrosion products include FeS, $Fe(OH)_2$, $CaCO_3$, and elemental sulfur (Starkey, 1985). $Fe(OH)_2$ and sulfur are corrosive to steel, and FeS is cathodic to metallic iron and increases corrosion (Starkey, 1985; Tiller, 1985). Iron tubercles form in aerobic systems due to the dissolution of iron by iron oxidizing bacteria (Tiller, 1985). Since particulate corrosion products affect the corrosion process, knowledge of their location and rate of movement is an important aspect of understanding microbially influenced corrosion.

Inorganic particles can also be formed by chemical precipitation. Such particles were found in biofilms grown on swine wastes after 4 to 12 months of growth (Harvey *et al.*, 1984; Robinson *et al.*, 1984). Energy dispersive X-ray analyses revealed the precipitates to be composed mostly of calcium and phosphorus. It was assumed that the precipitates formed in the biofilms and were not captured from the bulk liquid because of their presence on the substratum and surrounding some bacterial cells.

Particle movement due to advection has a direct effect on the population dynamics of the biofilm community. Particle advection in biofilms is due to the expansion of particulate volume as cells grow and EPS is formed. Advective velocity is most heavily influenced by the fastest growing microbial species, because this species creates the most particulate volume. Over time, a biofilm should become composed of greater concentrations of the fastest growing species, as the concentrations of slower growing species declines because of a limitation of space. Eventually, slowly growing microorganisms are pushed out the biofilm by faster growing cells. If population dynamics were determined by advection alone, only the fastest growing species would remain in a biofilm at steady state conditions. In a one-dimensional biofilm with only cell growth influencing particle transport, this species would be the one with the highest growth rate at the substratum (Gujer and Wanner, 1990).

Experimentation on biofilm population dynamics is difficult because significant spatial gradients exist in the chemical composition and population structure. Analysis of the interactions between the components of biofilm structure, and the processes occuring in a biofilm, requires maintenance of the intact structure in order to preserve the various gradients involved. The cellular structure and composition in biofilms are troublesome to study because of the minuscule spatial separations (on the order of micrometers) and the high volumetric density (ca. 10^{10} cells ml^{-1}).

Goal and Objectives

The goal of this research was to investigate particle-biofilm interactions, and to apply the results to further the understanding of biofilm population dynamics.

One objective was to develop an experimental technique that allowed detailed analysis of particle-biofilm interactions. The technique had to be able to differentiate particles from bacterial cells, determine spatial and temporal distribution of particles in biofilms, and permit quantification of particle concentrations in biofilm and bulk water. A second objective was to demonstrate capture and retention of micron-sized particles by biofilm. A third objective was to evaluate the capability of an existing biofilm model to simulate bead concentrations and distributions in biofilm, and to suggest possible improvements to the model.

LITERATURE REVIEW

Gradients in Biofilm Structure

Within biofilms are microbiological, chemical, and physical gradients that represent significant changes over distances of a few micrometers. Microbiological gradients represent changes in species composition and cell density in any dimension. Microcolonies within sludge granules have been revealed with immunologic methods (Grotenhuis *et al.*, 1991; Visser *et al.*, 1991), and microcolonies of different phenotypes in close proximity to each other present steep microbiological gradients. Chemical gradients are changes in chemical concentration in the interstitial water of the biofilm matrix. Dissolved oxygen (Lewandowski *et al.*, 1991) and nitrous oxide (N_2O) (Revsbech *et al.*, 1989) gradients have been measured with microelectrodes in studies of oxygen and nitrate respiration in biofilms. Variation in thickness and density represent physical gradients; thickness variations occur on a small spatial scale (Bakke, 1986).

All three categories of gradients are interrelated. Pores or crevices in biofilm cause changes in chemical composition by creating pathways for diffusion in biofilms without reaction (Wanner, 1989). Differing species composition across the substratum can cause changes in biofilm thickness

(Siebel and Characklis, 1991). Microbial activity strongly influences chemical gradients, both in depletion of substrates and production of products (sulfide, for example). Chemical gradients, in turn, regulate the environment and define where certain microbes may grow - aerobes where oxygen is present, or strict anaerobes in zones where oxygen is exhausted. Anaerobic conditions in biofilm depths often occur due to aerobic respiration in the biofilm nearer to the oxygen source.

Interactions between biofilms and viable and inert particles affect the various structures. Biofilm has been shown to enhance the capture of colloidal particles (Sprouse and Rittman, 1987). Filamentous surface structure, representing changes in physical and perhaps microbiological structure, may improve capture of particles from the bulk liquid (Alleman *et al.*, 1982). Particles may be substrates for microbial growth (Levine *et al.*, 1985) and thereby change substrate gradients and, indirectly, population gradients. If the particles are microbial cells or spores, new species may be introduced into biofilm, changing the microbiological structure, and introducing different activities that change the chemical structure.

Growth of different species in biofilms may alter biofilm structure and function. Particle movement in biofilms reflects competition for space by microbes, which may be important in biofilms (Atlas and Bartha, 1981). Some locations, such as adjacent to the substratum, have a special significance in population dynamics (Wanner, 1989). Therefore, the locations occupied by particles (cells) and the rate of change of the locations are indicative of shifts in population dynamics. However, making observations on processes such as particle movement in intact biofilm is difficult (Gujer and Wanner, 1990).

Mathematical Description of Biofilm Structure and Activity

Mathematical modelling is a necessary companion to experimentation in biofilm research because of the experimental difficulties inherent in taking measurements of gradients that exist on a scale of micrometers. Explicitly stating the conceptual model in mathematical terms aids in the separation of known facts from the assumptions required because of a lack of information. Because of difficulties in making observations on particle movement in biofilms, writing equations to describe particle movement does require some *a priori* assumptions about biofilm behavior.

Assumptions made to permit computation of particle movement include (Wanner, 1989):

- the volume fraction of solid phases is constant
- density (or, specific gravity) of the various solid phases to convert mass to volume units
- the displacement velocity for all particles located the same distance from the substratum is equal - that is, there is no variation across the substratum,

and no modelled attachment to the substratum

- movement occurs only in the dimension perpendicular to the substratum for one-dimensional models

An additional assumption commonly made in biofilm modelling is that all phenomena can be adequately described by a one-dimensional model of a uniformly thick biofilm.

Particle volume is created by the conversion of soluble substrates to cells and extracellular polymeric substances (EPS) during the growth of microbial cells. This conversion produces solid phase material (mass and volume). Space limitations in biofilm create an advection of particulates as new solid material is produced. Both the cell specific growth rate (μ) and the advective velocity (v) exist in gradients across the biofilm thickness (Figure 1). Advection is greatest near the biofilm-bulk water interface, because solid phase volume production between the substratum and the depth of interest must be included in the advection rate along with solid phase volume production at the depth of interest. The production of particulates normally causes a combination of film expansion and biofilm detachment. The rate of expansion (advection) equals the rate of biofilm volume produced per plan area of biofilm if advection is one-dimensional.

The change in concentration of solid components can be described by a one-dimensional mass balance (after Gujer and Wanner, 1990):

$$\frac{\partial \epsilon_s X_s}{\partial t} = -\frac{\partial J_s}{\partial z} + r_s \qquad (1)$$

where: X_s = particle concentration (M L^{-3})

ϵ_s = volume fraction occupied by a solid phase of the total biofilm volume (dimensionless)

J_s = flux of solid matter (M L^{-3} t^{-1})

r_s = reaction rate (production or degradation) (M L^{-3} t^{-1})

The change in soluble matter is described by a similar equation, which uses Fick's Law to predict the flux of material:

$$\frac{\partial \epsilon_l C}{\partial t} = D_f \frac{\partial^2 C}{\partial z^2} + r_{solute} \qquad (2)$$

where: C = concentration of solute (M L^{-3})

ϵ_l = volume fraction occupied by liquid of the total biofilm volume (dimensionless)

D_f = diffusion coefficient for solute in water in biofilm (L^2 t^{-1})

r_{solute} = reaction rate of solute (M L^{-3} t^{-1})

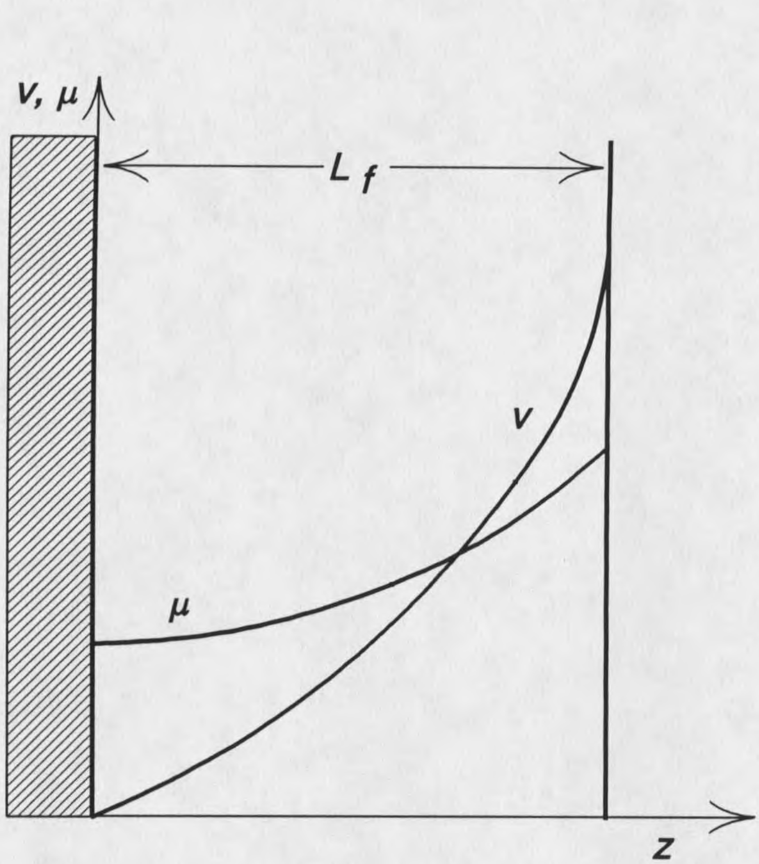

Figure 1. Typical gradients of specific cellular growth rate (μ) and advective velocity (v) over biofilm depth (L_f).

The creation of particle volume produces an advection of solid matter in the biofilm. A one-dimensional model such as BIOSIM (Reichert *et al.*, 1989) places all advection in the direction perpendicular to the substratum. However, the expansion of solids may fill in pores or the liquid occupied volume fraction of the biofilm as well as expanding the film away from the substratum. The advective flux is:

$$J_s = v_s X_s \tag{3}$$

where: J_s = advective flux of solids relative to the substratum (M L^{-2} t^{-1})

v_s = velocity of particle relative to the substratum (L t^{-1})

While diffusive-like transport of particles may be possible, it is normally assumed to be negligible (Gujer and Wanner, 1990; Stewart *et al.*, 1991; Kissel *et al.*, 1984).

Substituting equation (3) into equation (1) produces:

$$\frac{\partial X_s}{\partial t} = - v_s \frac{\partial X_s}{\partial z} - X_s \frac{\partial v_s}{\partial z} + r_s \tag{4}$$

Equation (4) may be solved with the following conditions (Gujer and Wanner, 1990):

- an initial condition that describes the profiles of the various particles over biofilm depth.
- a boundary condition of no flux at the biofilm-substratum interface:

$$\frac{\partial X_s}{\partial t}(z = 0, t) = 0 \tag{5}$$

Equation (2) requires a second boundary condition of continuity of concentration at the biofilm-bulk water interface:

$$C(z = L_f, t) = C_{bulk\,liquid}(z = L_f, t) \tag{6}$$

The advection of particulates (that is, cells) has been observed in immobilized cell reactors. Karel and Robertson (1989) used a radiotracer (^{35}S) to determine the location and rate of change of the bacterial growth region. Stewart *et al.*, (1991) measured growth region dimensions and cell growth rates with the same radiotracer and liquid emulsion radiography. Their experimental system was not a true biofilm because it entailed the placement of *Escherichia coli* on a microporous membrane, thus precluding cell detachment. While particulate advection has not been observed in biofilm systems, advection caused by cell growth has been theorized (Bryers and Characklis, 1982; Gujer and Wanner, 1990).

Applicability of the One-Dimensional Model

The model listed above is in a one-dimensional form. Although the model can be expanded to two or three dimensions (Gujer and Wanner, 1990), it is normally employed in the one-dimensional form (Reichert *et al.*, 1989; Kissel *et al.*, 1984). One-dimensional modelling considers gradients that exist in the dimension perpendicular to the substratum, but neglects any gradients parallel to the substratum. It is uncertain as to when the gradients parallel to the substratum are significant. Soluble substrate utilization appears to be insensitive to them, because one-dimensional models predict this phenomenon with good accuracy (Fruhen *et al.*, 1990; Gujer and Boller, 1990; Siegrist and Gujer, 1987). Other phenomena, such as particle capture and retention and population dynamics, involve particles with dimensions on the order of 1 to 10 μm. Heterogeneities in biofilm thickness, such as pores and crevices, exist at these and greater magnitudes, and may affect particle capture and retention.

The remainder of this thesis will show that variations in biofilm thickness across the substratum, such as pores, have a significant effect on particle capture and retention. Generalization of the results indicate that phenomena involving micron-sized particles, such as particle movement in biofilms, population dynamics, and particle detachment from biofilms, are poorly described by one-dimensional models because physical, microbiological, and chemical gradients exist across the substratum that determine the rates and magnitudes of changes in these phenomena.

EXPERIMENTAL SYSTEMS AND METHODS

Bacterial Characteristics

Pseudomonas aeruginosa, a rod-shaped chemoorganotroph, was used as the biofilm-forming species in all monopopulation biofilm experiments. It is motile by means of a polar flagella, and is obligately respiratory with oxygen or, in some circumstances, nitrate, as the terminal electron acceptor (Palleroni, 1984). A cell of this species is typically 1.5 to 4.0 μm long by 0.5 to 0.8 μm wide. *P. aeruginosa* have Gram negative cell walls. They form an extracellular polymer that consists mainly of mannuronic and guluronic acids (Evans and Linker, 1973). The optimum temperature range for this species is 35 to 37°C, with an optimal pH of 6.8.

Experimental System

Experiments were run in an annular reactor (RotoTorque) under turbulent flow conditions. A RotoTorque (RT) consists of a stationary vertical cylinder containing a co-axial rotating cylinder (Figure 2, Appendix A). Both cylinders are made of polycarbonate. The inner cylinder has four tubes at an angle from the axis so that the centripetal acceleration caused by rotation forces liquid up the angled tubes and thereby creates vertical mixing. The RT is a completely mixed reactor (Trulear 1980). Twelve removable slides for sampling of biofilm are set in dove-tailed vertical grooves in the outer cylinder, and are accessed through the top of the reactor through rubber-stoppered holes. The inner surface area of the reactor upon which biofilm can grow is 0.19 m^2.

The outer cylinder experiences a uniform shear stress since the annular gap is constant over the height of the reactor. Because the shear stress is uniform and the RT is a completely mixed reactor, it can be assumed that the biofilm growing on the outer cylinder is uniform in thickness and density, and that a biofilm specimen from any of the twelve slides (or, a portion of one of the slides) is a representative sample. The RT effluent is representative of the bulk fluid because the system is completely mixed.

Shear stress is dependent on the rotational speed of the inner cylinder, but is independent of the fluid flow rate. Shear stress and the hydraulic retention time can be controlled separately. The high surface area to volume ratio (Appendix A) provides adequate space for twelve slides while providing a short hydraulic retention time at relatively low flow rates. The rotational speed of the inner cylinder of the RT was 200 rpm in all experiments. The volume occupied by liquid at this rotational speed was 5.75×10^{-4} m^3.

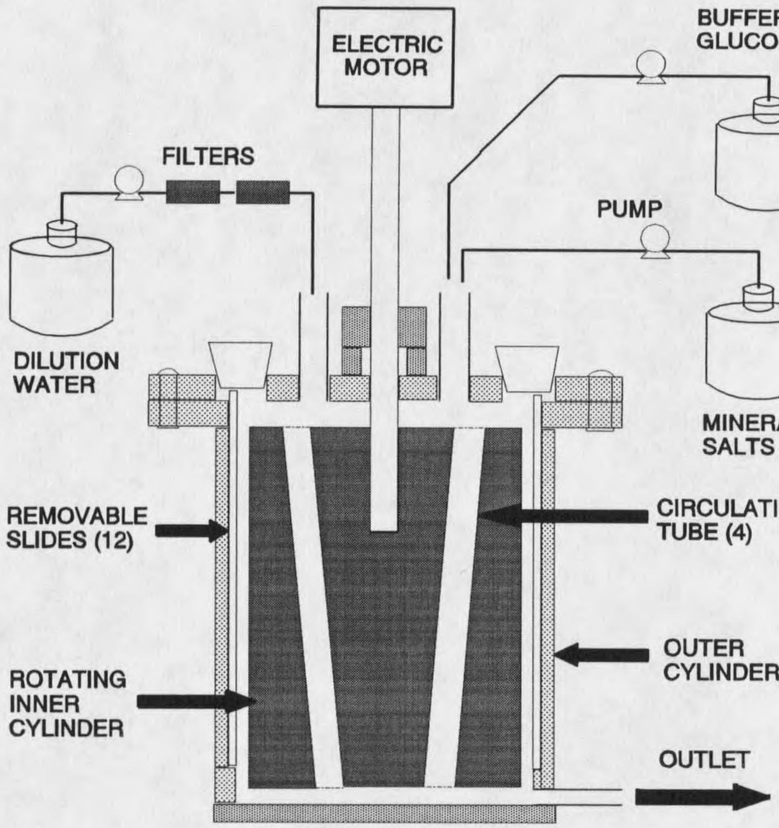

Figure 2. The RotoTorque reactor.

Experimental Procedures

Three separate flows were added to the RT. These summed to a flow rate of 0.0023 $m^3\ h^{-1}$ (38 ml min^{-1}), producing a hydraulic retention time of 0.25 h. At this retention time suspended bacteria are quickly washed from the RT and their activity can be neglected. The three component flows were mineral salts (5.8×10^{-5} $m^3\ h^{-1}$, or 1 ml min^{-1}), phosphate buffer (5.8×10^{-5} $m^3\ h^{-1}$, or 1 ml min^{-1}), and dilution water (0.0022 $m^3\ h^{-1}$, or 36 ml min^{-1}). Glucose was included with the phosphate buffer. Flow rates were measured with in-line flow meters (Gilmont Instrument Co., nos. 11 and 12). In addition, the total flow rate was determined once per day by measurement of the effluent volume in a graduated cylinder over a predetermined time, with the dilution flow rate adjusted to bring the total flow rate to 0.0023 $m^3\ h^{-1}$. Peristaltic pumps (Masterflex #7553-30, Cole-Parmer Instrument Co., with pump heads 7013 and 7014) were used to supply the dilution water, mineral salts, and buffer solutions.

Dilution water was taken from the Cobleigh Hall distilled water system. Three 0.02 m^3 (20 l) containers were filled daily. Water was transferred from container to container by siphons. The dilution water was aerated to ensure oxygen saturation before it was supplied to the RT. Sterilization of the dilution water was obtained by filtration through two 0.2 μm capsule filters (Gelman Sciences, Inc., #12122) in series.

The compositions of the mineral salts solution and the phosphate buffer solution are listed in Table 1. The medium was carbon limited according to the stoichiometry for *P. aeruginosa* growth on glucose (Characklis 1990a) and the dissolved oxygen concentration for water in equilibrium with the atmosphere at the elevation of Montana State University (Appendix B). Concentrated solutions (38x) were prepared in 0.011 m^3 (11 l) containers and autoclaved. In Experiments A-1, B-1, and A-2, the containers were autoclaved together for 50 min. After Experiment A-2, it was determined that this time period was inadequate for killing spores when such large liquid volumes were autoclaved. Thereafter, the two containers were autoclaved for a conditioning period of 0.17 h, a sterilization period of 3.3 h, and a slow exhaust period (variable). Glucose was added to a container by injecting 30 ml of concentrated glucose solution through a septum into the container. The glucose solution was filter-sterilized at the time of addition by passage through a 0.22 μm, 25 mm diameter nylon filter (Cameo IIS, Micron Separations, Inc.).

All experiments were run at 25$\pm$1°C. The RT was immersed in a water bath to a depth of 0.14 m. Approximately 0.75 m of the dilution water tubing was immersed in the water bath to adjust the dilution water temperature. The water bath temperature was controlled by a Yellow Springs Instrument Co., Inc. temperature controller (Model 74), or by a Fisher Scientific Co. Immersion Circulator (Model 730).

Table 1. Substrate solution compositions for the RotoTorque and chemostat reactors. All concentrations in g m^{-3}. The final pH is 6.8.

	RotoTorque	Chemostat
Glucose (Glucose - C)	15 (6)	100 (40)
NH_4Cl	7.2	36
$MgSO_4.7H_2O$	2.0	10
$(NH_4)_6Mo_7O_{24}.4H_2O$	0.001	0.005
$ZnSO_4.7H_2O$	0.1	0.5
$MnSO_4.H_2O$	0.008	0.04
$CuSO_4.5H_2O$	0.002	0.01
$Na_2B_4O_7.10H_2O$	0.001	0.005
$FeSO_4.7H_2O$	0.112	0.56
$(HOCOCH_2)_3N$	0.4	2.0
$CaCO_3$	-	1.0
$CaCl_2.2H_2O$	11.0	-
Na_2HPO_4	213	568
KH_2PO_4	204	544

Reactor Start-up

The RT assembly (including connecting tubing, with silicone tubing used exclusively, flowmeters, flow breaks, and dilution water filters) was autoclaved for 0.33 h. All open tube ends were covered by aluminum foil. Water (about 20 ml) was placed inside the RT before autoclaving in order to provide moist heat for the sterilization.

Connections were made to the mineral salts and phosphate buffer containers by heating a borosilicate glass tube connector with a propane torch until its end was red hot, then pushing the glass connector into the silicone tubing attached to a container. The RT was filled with the nutrient and buffer solutions and dilution water in the correct proportion. Adequate care was necessary to release trapped air from the RT. The inner cylinder rotation was initiated. Chemostat effluent (5.8×10^{-5} m^3 h^{-1} (1 ml min^{-1}), cell concentration was 5 to 7 x 10^7 cells ml^{-1} for a *P. aeruginosa* flow rate of 4 x 10^9 cells h^{-1}) was added to provide an inoculum of the desired species. This inoculation period lasted 12 h (total flow rate of 0.0023 m^3 h^{-1} (38 ml min^{-1}), dilution water flow rate of 0.0021 m^3 h^{-1} (35 ml min^{-1})), at which time the chemostat was disconnected from the RT.

One experiment was run with an undefined, mixed population biofilm. Non-sterile, unfiltered water from the Engineering Research Center's reverse osmosis treatment system (cell concentration of 1.1 x 10^6 ml^{-1}) was the inoculum source. This water was used in place of dilution water for 48 h during the RT inoculation. At that time, filtered, sterile distilled water replaced the unfiltered reverse osmosis system water as dilution water, and bead addition was begun. Bead addition took place for 24 h. The system was monitored for 144 h after the end of bead addition. A homogenized biofilm sample taken at 24.3 h after the end of bacteria inoculation was streaked onto R2A agar supplemented with glucose, and bacteria from the three predominant colony morphologies were characterized (Table 2).

Table 2. Bacteria characteristics of the three predominant colony morphologies (yellow, white, and small colonies) in experiment MP-1.

	Colony Morphology		
Characteristic	yellow	white	small
Gram stain	-	-	-
cell morphology	rod	short rod	short rod
motility	-	+	+
oxidase test	+	-	+
colony diameter (mm)	7-8	7-8	2-3
colony shape	round	round	round

Sampling

Effluent was grab sampled daily. Approximately 75 ml of effluent was collected in a sterile 250 ml beaker. A subsample was taken for glucose analysis; it was filtered through a 0.2 μm membrane filter to remove cells and then frozen. The remaining sample was homogenized with a Tekmar Tissuemizer for 90 sec at 90% power. A subsample was removed for cell enumeration and was preserved in 2% formaldehyde and refrigerated until analysis. Another subsample for TOC analysis was acidified with concentrated phosphoric acid to a pH less than 2 and frozen until analysis. Subsamples for bead counts were refrigerated.

Biofilm samples were obtained from the removable slides in the RT. Before slide removal, the area around the stopper to be pulled was dosed with 70% ethanol. After approximately 2 min, the ethanol was ignited, and after the flame was extinguished, the stopper was removed and stored in 70% ethanol. The slide was pulled out with a needle nose pliers which had been disinfected with 70% ethanol (residual ethanol burned off before sampling). Residual ethanol was burned off of the stopper before its replacement in the top of the RT. On some samples, biofilm thickness was measured. Biofilm was scraped off of a measured area on a slide into sterile 3 mM phosphate buffer (variable volume, from 5×10^{-5} to 1×10^{-4} m^3 (50 to 100 ml)). This mixture was homogenized with the Tissuemizer for 5 min at 90% power. Subsamples for cell counts, bead counts, and TOC were handled as described for effluent samples.

Microbead Characteristics

Latex microbeads used in these experiments (Polysciences, Inc., #15702) were chosen to simulate the physical characteristics of a bacterial cell. Their properties include (1) a nominal diameter of 1 μm, (2) a specific gravity of 1.05, and (3) a negative surface charge due to the incorporation of carboxyl groups during bead manufacture. The microbeads contained a fluorescent dye which made them easy to distinguish and enumerate under the microscope. The beads were suspended in distilled water or 0.85%

NaCl solutions and autoclaved (20 min) before their addition to the annular reactor, with the exception of Experiment A-2, where the beads were sterilized by glutaraldehyde (1%, 1 h contact time), and separated from the glutaraldehyde through centrifugation. Microbeads were added to the RT at a flow rate of 5.8×10^{-5} m^3 h^{-1} (1 ml min^{-1}) for 24 h. The point in the experiment when the microbeads were added varied (Table 3).

Table 3. Experimental protocols.

Experiment	initiation of bead addition[1]	length of bead addition period (h)	total experiment duration (h)	bulk liquid bead concentration during bead addition (# m^{-3})	fraction of beads which attached
A-1 (nascent)	0	24	144	3.9×10^{13}	0.0013
A-2 (nascent)	0	24	144	8.9×10^{12}	0.0038
B-1 (mature)	120	24	264	3.9×10^{12}	0.012
B-2 (mature)	120	24	264	2.9×10^{12}	0.010
B-3 (mature)	120	0.14	216	7.2×10^{14}	0.100
MP-1 (nascent)	0	24	168	-	-

[1] Hours after the end of bacterial inoculation.

According to the manufacturer (personal communication), latex microbeads are composed of polystyrene, with trace amounts of carboxylate groups, a fluorescent dye, and a surfactant to allow the dye to be incorporated in the non-water soluble matrix. The polymers are not crosslinked. Carboxylate groups are at a concentration of 1 to 10 parts per million. A monomer containing these groups is added after the beads are made but some groups do diffuse into the polystyrene matrix. Therefore, the negative charges are not located solely on a bead surface. The carboxylate groups are tightly bound to the polystyrene; fluctuation of charges over time does not occur. Polystyrene and attached carboxylate groups are not biodegradable in the time periods covered by the experiments. Also, the beads are not affected by glutaraldehyde or formaldehyde.

Chemostat Reactor

A chemostat is a continuously flowing stirred tank reactor in which bacteria are grown. A chemostat was used in these experiments to inoculate the RT. This was done to standardize, as much as possible, the initial conditions in order to aid modelling and improve comparisons between duplicated experiments.

The composition of the chemostat influent solution is given in Table 1. Since the solution was oxygen limited, filtered air was sparged into the chemostat to increase the bacterial concentration.

The chemostat, accessory tubing, flowmeter, air filter, and 0.006 m^3 (6 l) of chemostat medium were autoclaved together for 0.83 h. After the problem with the spores was discovered, the autoclave time was increased to 1.5 h. Glucose and calcium carbonate were added to the medium by injection through a septum with filter sterilization after autoclaving. The chemostat was inoculated with approximately 0.5 ml of a frozen cell suspension of *P. aeruginosa*. The broth was run in a batch mode (zero flow rate) for 8-12 h, by which time it had become turbid. The chemostat was then run at a dilution rate (flow rate divided by reactor volume) of 0.125 h^{-1} (5.8×10^{-5} m^3 h^{-1}) for 24 h (3 retention times) to produce a steady state cell concentration before the RT inoculation began.

The chemostat temperature was not controlled. Ambient temperatures ranged from 20-26°C.

Analytical Methods

Cell counts. All cell counts were total direct counts (Hobbie *et al.*, 1977). Samples (variable volumes) were added to an equal volume of Hoechst 33342 stain (100 μM), vortexed, and stored in the dark for 1 to 24 h. The samples, or an aliquot, were filtered through a 0.2 μm black membrane filter and observed under an Olympus BH-2 microscope using epifluorescent light. Cells were counted by an image analysis computer program using either a Cambridge/Olympus hardware and software package or an American Innovision package. The image analysis systems also provided average cell area. Cell concentrations and cell area were converted to cell carbon equivalents (Bakke *et al.*, 1984).

Microbead counts. The fluorescent microbeads were counted with a procedure similar to that used for cells. The samples were not fixed in formaldehyde, and no fluorescent stain was necessary.

Total Organic Carbon (TOC). TOC was determined on a Dohrmann DC-80 Carbon Analyzer according to the directions of the manufacturer.

Soluble Organic Carbon (SOC). The sample was centrifuged for 0.25 h at 20,000 rpm. The tubes had been washed in Micro™ soap and hot water, and then rinsed three times each in tap, distilled, and ultrapure water. The supernatant was analyzed for total carbon as described above.

Dry density. A measured area of biofilm was scraped into a pre-weighed aluminum dish. The sample was dried at 96°C for at least 3 h, cooled in a dessicator, and weighed. Areal density was calculated as the quantity of dried solids divided by the area scraped. Volumetric density was calculated as the areal density divided by the biofilm thickness.

Glucose. Glucose was determined by a colormetric enzymatic method (Sigma Diagnostic, #510-A). The method employed was similar to the Sigma method, with the exception being that 2.5 ml of sample was used instead of 0.5 ml because of the relatively low glucose concentrations.

Biofilm thickness. Two methods were used to measure biofilm thickness. The more frequently used method was observation by light microscopy at 400x. The difference in the vernier on the fine focus knob between focusing on the biofilm surface and on the biofilm-substratum interface was noted, with the difference being read directly in μm (Trulear and Characklis, 1982). Optical thickness was multiplied by 1.33 to determine mechanical thickness (Bakke and Ollsen, 1986). For two samples in Experiment B-1, thickness was measured by a displacement of water method (van der Wende, 1991). This technique gave average film thickness in one measurement, and did not give any information on variation in film thickness.

Microscopy of cross-sections. In experiments where samples for sectioning were taken, polycarbonate membranes were taped to RT slides. After the slides were removed from the RT, the biofilm-membrane specimens were fixed in glutaraldehyde (2.5% glutaraldehyde in phosphate buffered saline), dehydrated in ethanol, and embedded in JB-4 plastic (Polysciences, Inc., #18570). Other fixatives were tried besides glutaraldehyde (paraformaldehyde, formaldehyde, and cationic ferritin in combination with each of the three aldehydes), but the procedure described above worked the best. Thin sections (2.5 µm) were cut from the plastic blocks with a microtome using a glass knife, and the sections stained with Giemsa stain to highlight the bacteria.

The thin sections were examined and photographed with an Olympus BH-2 microscope using simultaneous transmitted white and epifluorescent light. Distance measurements from the thin cross-sections were made with the Olympus microscope and an American Innovision Videometric 150 image analysis system. Microbead profiles were constructed from distances measured on thin cross-sections with the American Innovision Videometric 150 image analysis system. Distances were measured along a normal to the substratum to beads (z) and to the biofilm-bulk water interface (L_f) where beads were located (Figure 3). Ratios of distance to beads over distance to the biofilm-bulk water interface were normalized to an average biofilm thickness (z^*):

$$z^* = \frac{z}{L_f} * L_f^* \tag{7}$$

where L_f^* is a biofilm thickness averaged over space and time for the period covered by the profiles. Absolute and normalized bead locations were grouped into 1 µm intervals, and the frequencies converted to concentrations using the independently-measured areal bead concentrations.

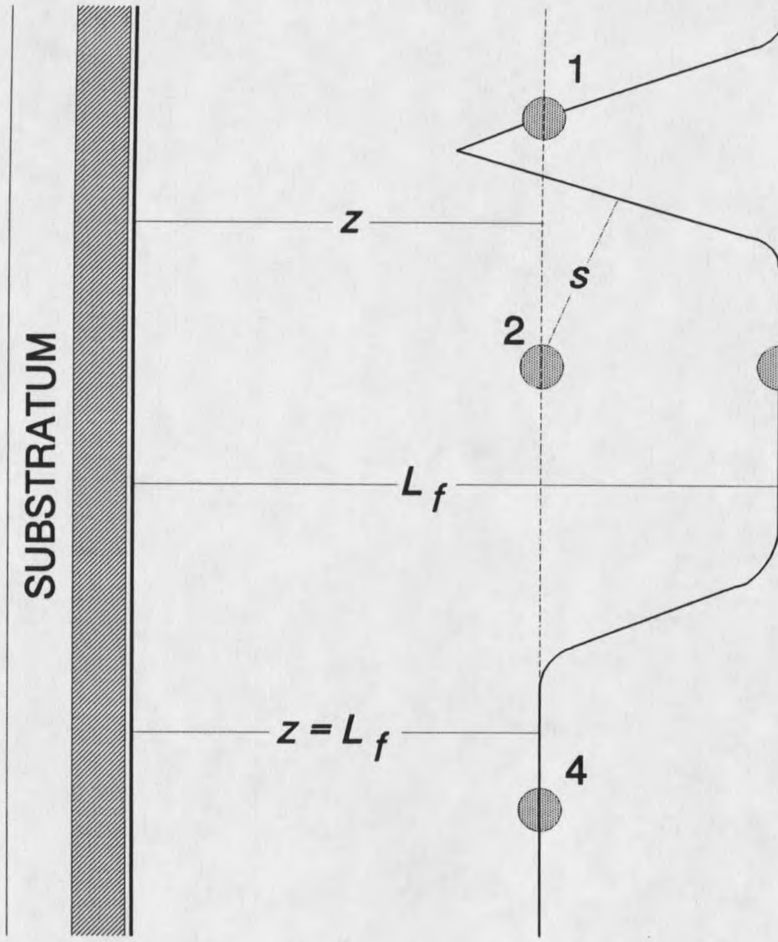

Figure 3. Schematic of bead position measurements. The substratum is on the left; the biofilm surface on the right. The distance between the substratum and beads (z) is less than or equal to the distance between the substratum and the biofilm surface (L_f). All measurements (except s) are perpendicular to the substratum.

Microbead aggregation studies. Microbead aggregation in biofilm and bulk water was assessed using the Hopkins statistic nearest-neighbor analysis for clustering (Jain and Dubes, 1988). Clean microbeads were mixed with RotoTorque effluent for 0.25 h (one residence time in the reactor), then filtered on to a 0.2 μm black membrane filter. The filters were observed microscopically with ultraviolet light, and bead locations were determined in a Cartesian coordinate frame with the American Innovision image analysis system. Hopkins statistics were determined for ten fields per filter, with the ten values from each filter being averaged. Four treated samples and one no-treatment control (beads without reactor effluent) were analyzed. Hopkins statistics were similarly determined for two biofilm samples. These samples were observed by phase contrast microscopy, with coordinates determined for a total of three fields.

RESULTS

The interaction of microbeads with biofilm was studied in two experimental designs. Microbeads were added to either nascent (Type A experiments) or mature (Type B experiments) *P. aeruginosa* biofilms, or a nascent undefined mixed population (MP-1) biofilm. Nascent biofilms were thin (approximately 2 μm for *P. aeruginosa*, an average of 17 μm for the mixed population biofilm) with only partial surface coverage, while a mature *P. aeruginosa* biofilm had reached its maximum average thickness (approximately 35 μm) with complete surface coverage. The biofilm reactor was operated for 96 to 144 hours after the end of bead addition, during which time the biofilm was sampled to determine the number and distribution of beads in the biofilm. Experimental protocols are summarized in Table 3. Data on areal biofilm concentrations (microbeads, cells, TOC, EPS, biofilm thickness) and reactor effluent concentrations (microbeads, cells, EPS, TOC, and glucose) are listed in Appendix C. Microbead profile data are in Appendix D.

Microbeads added in aqueous suspension to the reactor attached to the biofilm. The fractions of attaching microbeads ranged from 10^{-3} to 10^{-1} and are reported in Table 3. The fractions were calculated as the number of microbeads attached to biofilm at the end of the bead addition period divided by the number of beads delivered to the reactor.

Individual microbeads attached to biofilm were readily identified and distinguished from bacteria. Section views indicated that beads were located within the biofilm (Figure 4). Beads were also observed in the biofilm interior by phase contrast microscopy and scanning confocal laser microscopy. Beads can be identified at relatively low magnification (125x) when fluorescing, giving sensitivity to the identification and counting process. Counting of individual beads directly on the slides (plan view) was not always possible because of the presence of some bead aggregates.

Biofilm microbead concentrations decreased over time. The progression of microbead concentrations in experiments A-1, A-2, B-1, and B-2 is presented in Figure 5. Data for Experiment B-3 are not shown, since those concentrations are an order of magnitude greater than the concentrations for the other experiments. Areal bead concentrations in the mixed population biofilm experiment remained constant throughout the experiment (Appendix C).

Microscopic examination of thin cross-sections from the nascent biofilm experiment A-1 indicated that microbeads were located near the substratum at 48 h after the end of bacterial inoculation and were still near the substratum at 144 h (Figure 6). Quantitative measurements of bead positions from cross-sections also revealed skewed distributions, with bead concentrations decreasing toward the biofilm-bulk water interface (Figure 7).

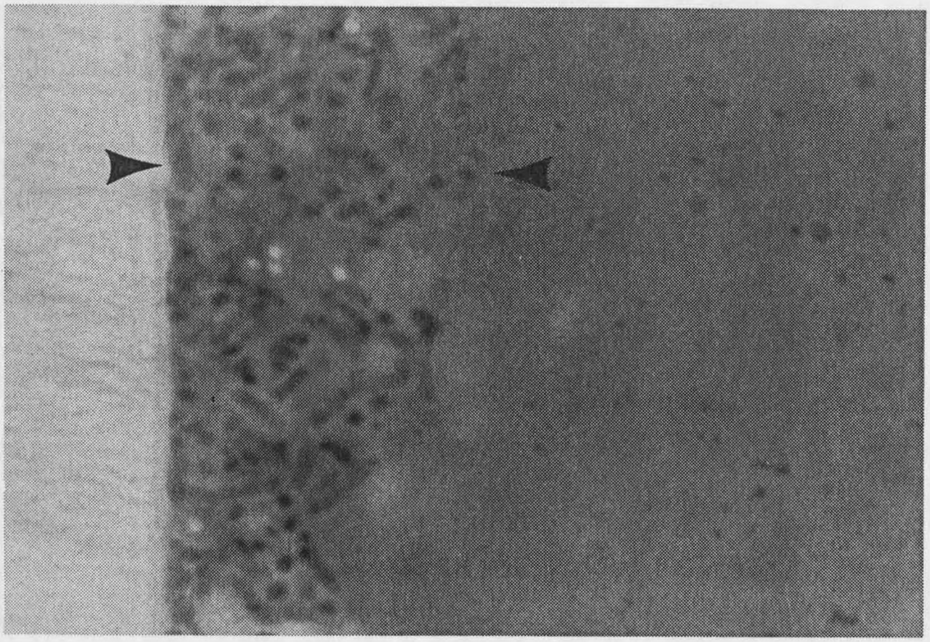

Figure 4. Biofilm cross-section from 144.75 h in Experiment B-2. The sample was taken 45 minutes after the cessation of microbead addition. Microbeads had effectively penetrated the entire biofilm thickness.

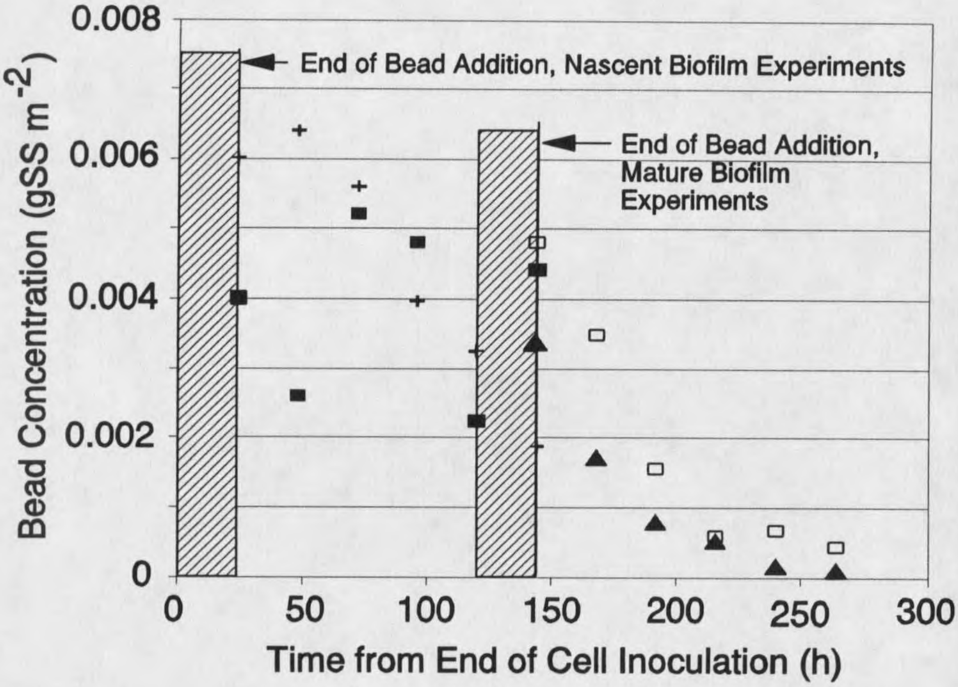

Figure 5. Biofilm microbead concentrations versus time for the nascent and mature biofilm experiments. The shaded regions indicates the bead addition periods. Experiment A-1 (+); A-2 (■); B-1 (□); and B-2 (▲).

The profiles also indicate that bead concentrations decreased over time. The change in bead concentration near the substratum was equal to the rate of dilution by cell growth and EPS production. The growth rate is given by:

$$\mu = \frac{-\ln \frac{X_{f,2}}{X_{f,1}}}{t_2 - t_1} \tag{8}$$

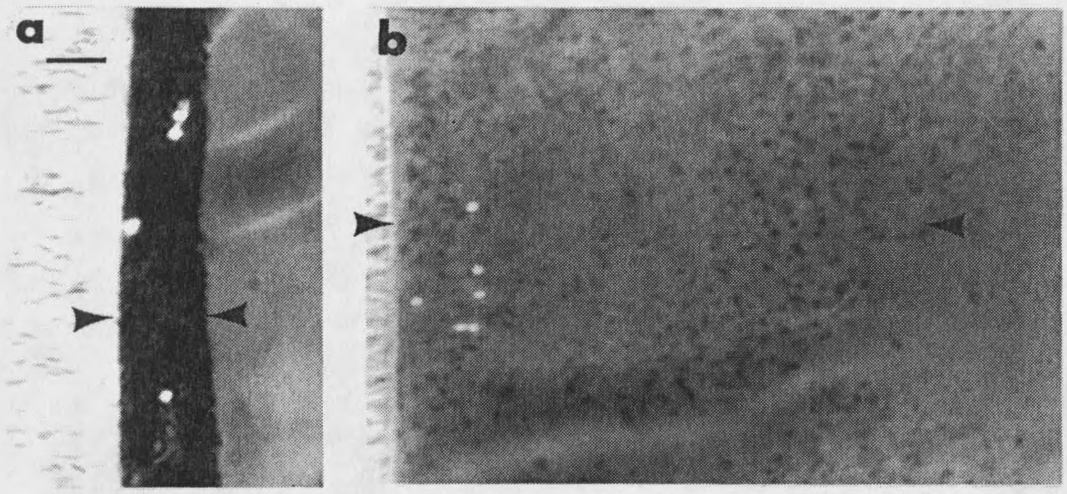

Figure 6. Biofilm cross-sections from Experiment A-1. The microbeads are approximately 1 μm in diameter. (a) Section from 48 h after the end of bacteria inoculation. The bacteria (dark particles) have grown over and entrapped the microbeads (light particles). Bar = 5 μm. (b) Section from 144 h. The remaining microbeads were generally located near the substratum. The dark areas in (a) and (b) are wrinkles produced during manufacture of the cross sections.

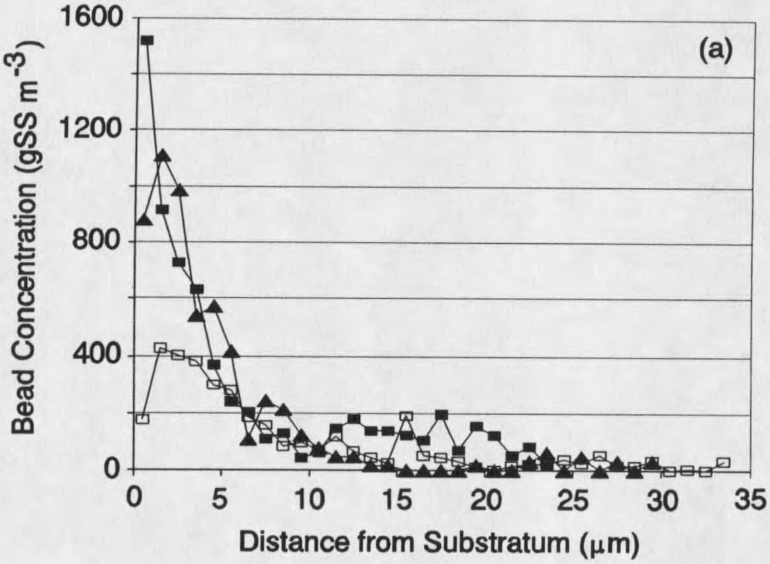

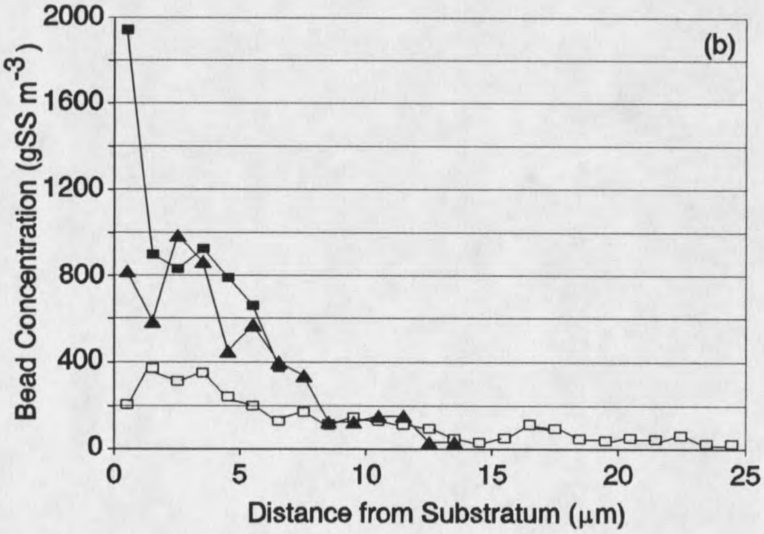

Figure 7. Bead profiles in the biofilm at 48 (■), 72 (▲), and 120 (□) h after cell inoculation in experiment A-1. The end of bead addition was at 24 h. (a) Unaltered profiles of bead concentrations. (b) Bead profiles normalized to the local biofilm thickness and then scaled to average film thicknesses of 7, 14, and 25 μm, respectively.

where: μ = biomass growth rate measured from bead dilution rate (t^{-1})

X_f = volumetric bead concentration ($M\ L^{-3}$)

1,2 = subscripts denoting consecutive times

The calculated rate (μ) was 0.028 h^{-1} for the beads in the first micrometer next to the substratum over the 72 hour period covered by the profiles.

Thin sections from the mature biofilm experiment B-2 show microbeads located throughout the depth of the biofilm 0.75 h after the end of microbead inoculation (t = 144.75 h) (Figure 4). The 168.6 h profile has concentrations similar to the 144.75 h profile at the substratum (Figure 8a). Most of the microbeads were located near the biofilm-bulk water interface at the earlier time, but later in the experiment (24.6 h after bead addition, or t = 168.6 h) a larger fraction of the beads was nearer to the substratum (Figure 8b).

In the mature biofilm experiment B-3 (pulse bead addition), beads were associated primarily with the biofilm-bulk water interface immediately after bead addition. The biofilm surface was irregular, with pores or crevices. The pores usually contained beads (Figures 9a, 9b). Therefore, beads were located at different distances from the substratum. At 8.9 h after bead addition (t = 128.9 h), several layers of bacteria covered most of the beads (Figure 9c). Beads were located even farther away from the biofilm-bulk water interface as time progressed (Figure 9d). Absolute-distance bead profiles show little change between 120.05 and 128.9 h, with

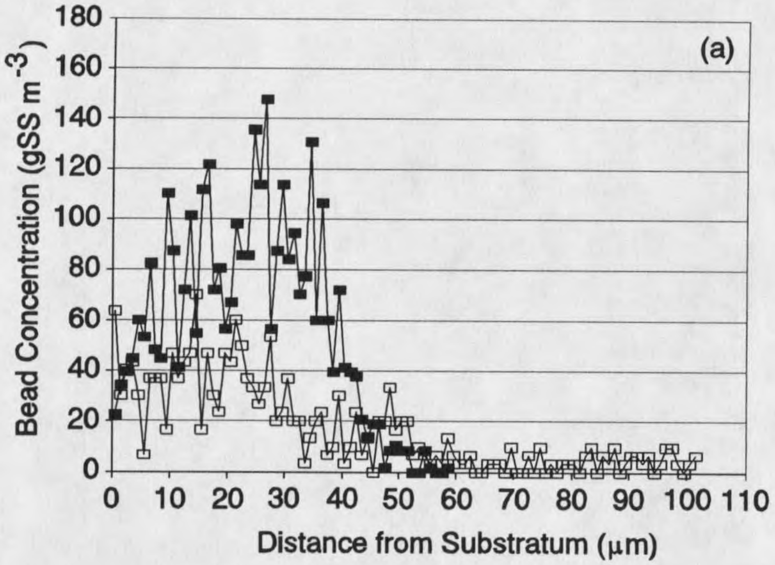

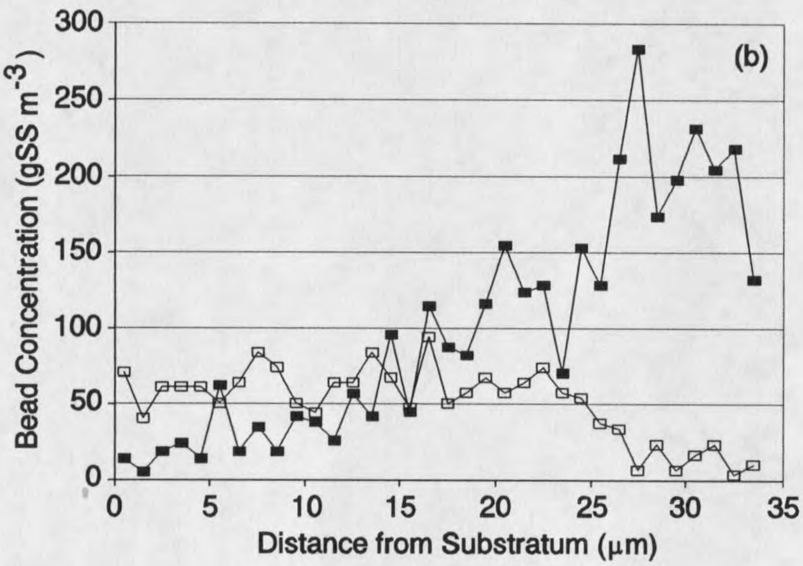

Figure 8. Bead profiles in the biofilm at 144.75 (▪) and 168.6 (▫) h after cell inoculation in experiment B-2. The end of bead addition was at 144 h. (a) Unaltered profiles of bead concentrations. (b) Bead profiles normalized to the local biofilm thickness and then scaled to an average thickness of 34 μm.

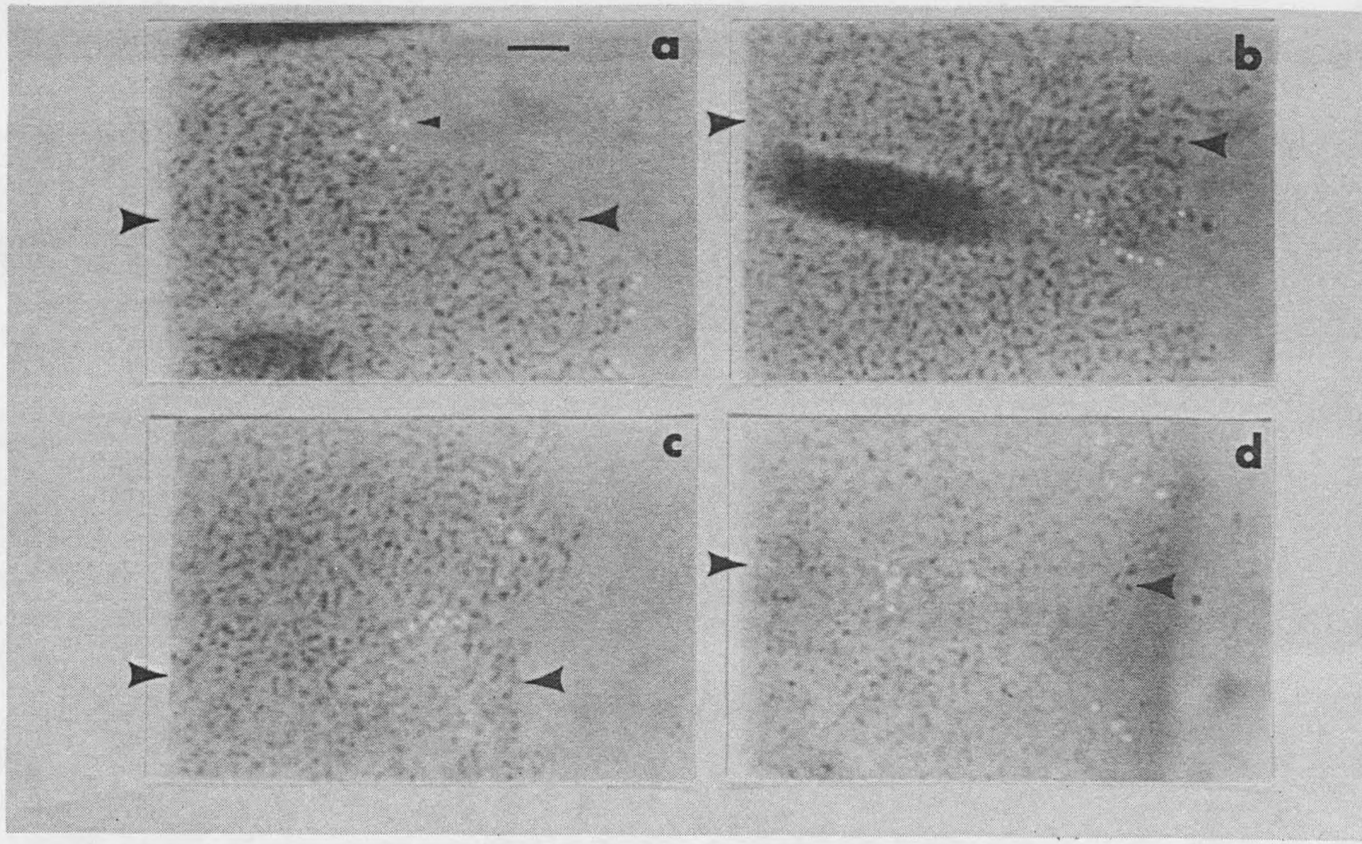

Figure 9. Biofilm cross-sections from Experiment B-3. (a) At 120.05 h, microbeads are at the biofilm-bulk water interface, including pore interfaces. Small arrowhead = bead; large arrowhead = biofilm surface. Bar = 5 μm. (b) Also at 120.05 h, another view of how pores provide a conduit for particle movement into a biofilm. (c) Microbeads are in the interior of the biofilm and not associated with an interface at 128.9 h. (d) Much of the biofilm thickness contains microbeads at 143.9 h.

higher bead concentrations near the substratum at 143.9 and 191.9 h (Figures 10a and 11a). Profiles normalized to a thickness of 37 μm indicate that bead concentrations near the biofilm-bulk water interface decreased over time, but increased over time near the substratum (Figures 10b and 11b).

A bead profile was constructed from scanning confocal laser microscope (SCLM) images. This profile, from four scans of a biofilm sample from experiment B-3, has a mode in approximately the same location as profiles made from cross-sections from the experiment (Figure 12). However, the peak bead fraction in the SCLM profile is twice that of the cross-section profiles, and the distribution is narrower. Artifacts due to sample handling should be less in the SCLM profile, because that sample was not fixed, dehydrated, sliced, or stained. A difficulty encountered in preparation of the SCLM profile was overlapping "halos" around the beads prevented counting of individual beads in the SCLM images, and caused transference of bead images to neighboring horizontal sections. Beads were quantified by the area they illuminated. Determination of the area due to beads truly in a horizontal section, and not from bead halos in other sections, required judgement. Also, vertical movement of the microscope stage had not been calibrated at the time the SCLM scans were made, and it is possible that the biofilm thickness reported to be scanned was not accurate. Therefore, the SCLM profile was normalized to the maximum thickness obtained from the cross sections (41 μm). Uncertainty exists in the profiles from both the SCLM images and the cross-section samples, due to unfamiliarity with SCLM optimization and sample preparation and handling for the cross-sections. Similarity in the profiles indicates that artifacts in the profiles from cross-sections are not pronounced.

In experiment MP-1, beads were generally near the substratum at 80.6 h after the end of bacteria inoculation (Figure 13a). However, at 142.4 h, the beads were dispersed throughout the thick biofilm (Figure 13b).

The percentage of beads at the biofilm-bulk water interface decreased rapidly in the first 3 hours after bead addition in experiment B-3 (Figure 14). This decrease continued at a lesser rate for the next 21 hours. The numbers of beads within 3 μm of the biofilm-bulk water interface decreased in a similar pattern.

Bead aggregation was evaluated using the Hopkins statistic. With this measure, a value of 0.5 represents a random distribution of points, whereas values near 1.0 indicate that aggregation has occurred. The Hopkins statistic values for all bulk liquid samples, including the control, ranged from 0.60 to 0.63, with standard deviations in the ten analyses per filter ranging from 0.059 to 0.14 (Appendix E). Because the statistics are near 0.5 and the values for the treated samples equal that of the control, no bead aggregation occurred in these tests. The small amount of aggregation indicated by the values of 0.6 was most likely an artifact created during

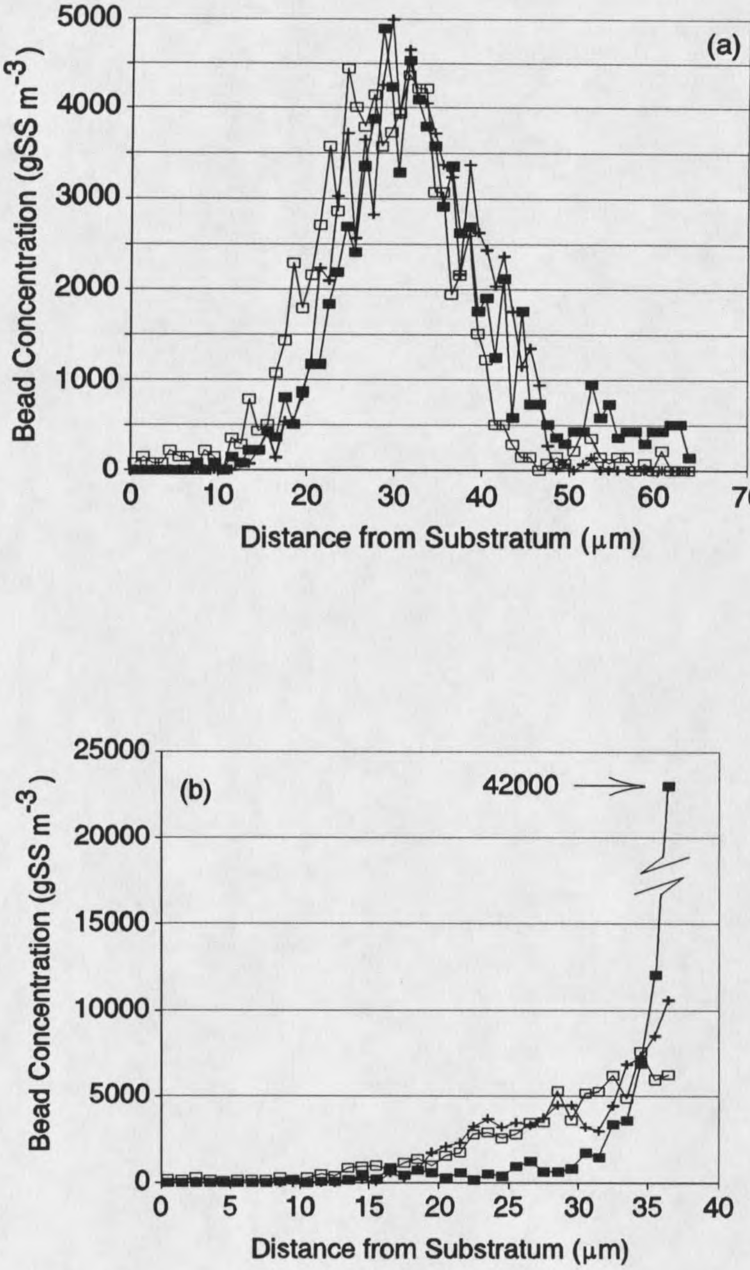

Figure 10. Bead profiles in the biofilm at 120.05 (■), 122.9 (+), and 128.9 (□) h after cell inoculation in experiment B-3 (pulse bead addition). The end of bead addition was at 120 h. (a) Unaltered profiles of bead concentrations. (b) Bead profiles normalized to the local biofilm thickness and then scaled to an average film thickness of 37 μm.

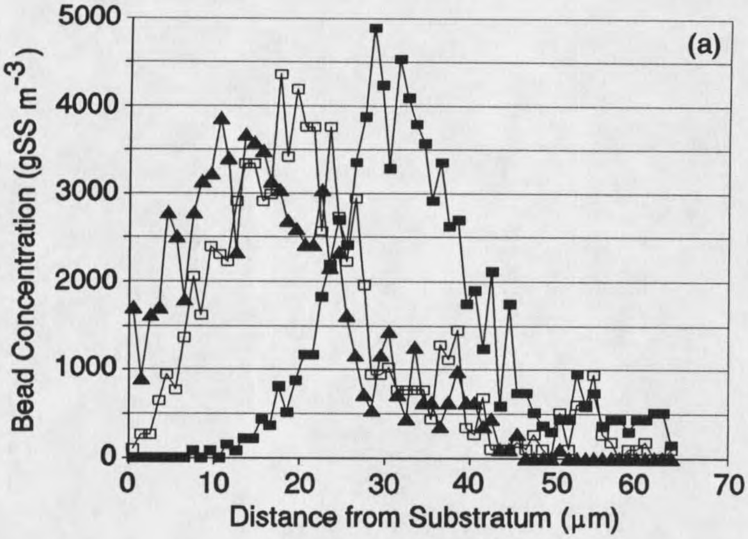

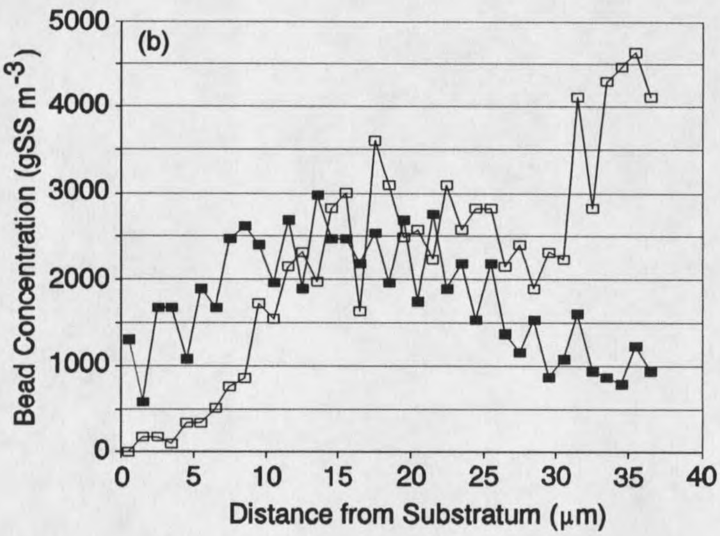

Figure 11. Bead profiles in the biofilm at 120.05 (■), 143.9 (□), and 191.9 (▲) h after cell inoculation in experiment B-3 (pulse bead addition). The end of bead addition was 120 h. (a) Unaltered profiles of bead concentrations. (b) Bead profiles normalized to the local biofilm thickness and then scaled to an average film thickness of 37 μm. The normalized profile at 120.05 h is not shown in (b).

filtration by imperfections in the filters. Biofilm samples, in contrast, had Hopkins statistic values ranging from 0.93 to 0.98. Therefore, beads did aggregate in or on the biofilm.

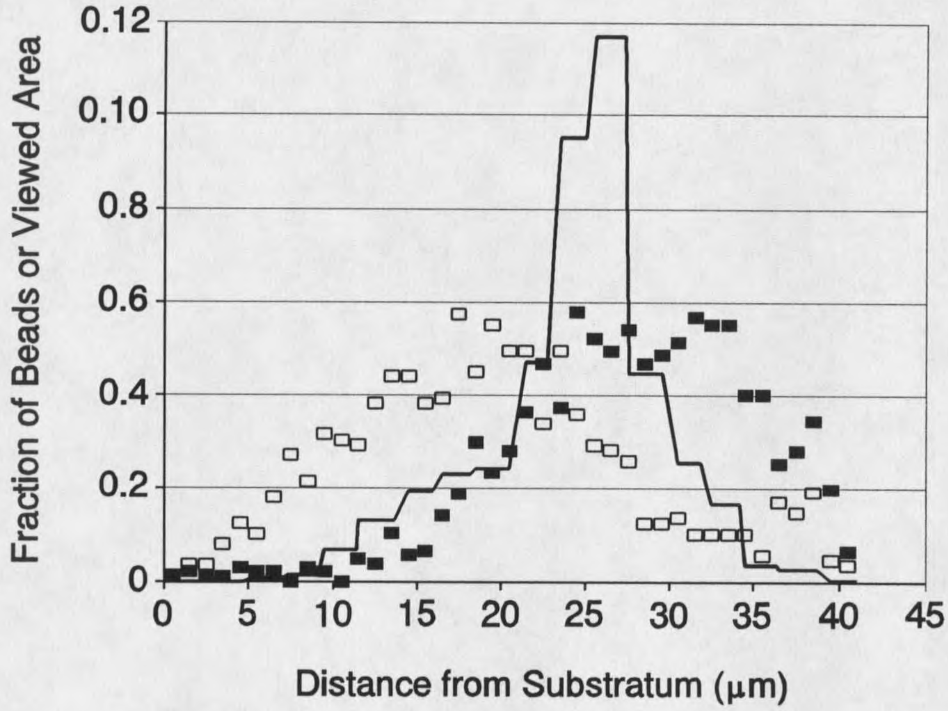

Figure 12. Bead profiles by scanning confocal laser microscope at 136.9 h (———) and from embedded, sliced cross-sections at 128.9 (▪) and 143.9 (▫) h. Both the peak locations and shapes of the profiles are similar.

Biofilm thicknesses for the nascent and mature *P. aeruginosa* biofilm experiments are shown in Figure 15. The mixed population biofilm had a large variation in thickness (Figure 16), with an average thickness an order of magnitude greater than the *P. aeruginosa* biofilms. Biofilm thicknesses measured at distinct points on a given sample vary significantly, suggesting